Consiglio Nazionale delle Ricerche
Istituto di Calcolo e Reti ad Alte Prestazioni

Properties determining parameters choice in meshless solver for electromagnetic transients

G. Ala, E. Francomano, A. Tortorici, E. Toscano, F. Viola

Rapporto Tecnico N.:
RT-ICAR-PA-06-09

novembre 2006

Consiglio Nazionale delle Ricerche, Istituto di Calcolo e Reti ad Alte Prestazioni (ICAR)
– Sede di Cosenza, Via P. Bucci 41C, 87036 Rende, Italy, URL: *www.icar.cnr.it*
– Sezione di Napoli, Via P. Castellino 111, 80131 Napoli, URL: *www.na.icar.cnr.it*
– Sezione di Palermo, Viale delle Scienze, 90128 Palermo, URL: *www.pa.icar.cnr.it*

Consiglio Nazionale delle Ricerche
Istituto di Calcolo e Reti ad Alte Prestazioni

Properties determining parameters choice in meshless solver for electromagnetic transients

G. Ala[3], E. Francomano[1,2], A. Tortorici[1,2], E. Toscano[1,2], F. Viola[3]

Rapporto Tecnico N.:
RT-ICAR-PA-06-08 **novembre 2006**

[1] Istituto di Calcolo e Reti ad Alte Prestazioni, ICAR-CNR, Sezione di Palermo Viale delle Scienze edificio 11 90128 Palermo
[2] Università degli Studi di Palermo Dipartimento di Ingegneria Informatica Viale delle Scienze, edificio 6, 90128 Palermo
[3] Università degli Studi di Palermo Dipartimento di Ingegneria Elettrica, Elettronica e delle Telecomunicazioni, Viale delle Scienze, 90128 Palermo

Abstract: In this paper some key elements of the Smoothed Particle Hydrodynamics methodology suitably reformulated for analyzing electromagnetic transients are investigated. The attention is focused on the interpolating smoothing kernel function which strongly influences the computational results. Some issues are provided by adopting the polynomial reproducing conditions. Validation tests involving Gaussian and cubic *B*-spline smoothing kernel functions in one and two dimensions are reported.

Keywords: meshless particle method, Smoothed Particle Hydrodynamics method, Maxwell's equations, electromagnetic transients.

1. Introduction

In the last two decades the meshless methods have known a great success in the simulation of a wide variety of applications as a valid computational alternative to grid methods. They share common features such as the avoidance of the use of grids, but are different in the means of function approximation and computational process.

The numerical technique known as Smoothed Particle Hydrodynamics (SPH) [4]-[6], [10], [11] is a meshless method and its attractiveness and popularity is due to the evaluation of unknown field functions and relative differential operators by means of an integral representation based on a suitable interpolating function. The integral representation is discretized by using a set of *particles* scattered in the problem domain.

The appropriate choice of the *smoothing kernel function* is a crucial task before performing any calculation using the SPH solver. The smoothing kernel function is of remarkable importance since it not only determines the interpolating pattern, but also defines the width of the influence area of a particle determined by a parameter h called as *smoothing length*. The choice of this parameter is a key variable for the kernel's worth. In fact, the smoothing kernel function should have a certain degree of consistency which can be expressed by its ability to reproduce the polynomials in both the integral and discrete formulations [2], [3], [7]. For each smoothing kernel function only a set of h values, related to the interspacing particles, verifying the polynomial reproducing conditions must be taken into account. In this paper an analysis of the smoothing length h values is carried out by adopting two bell-shaped smoothing kernel functions widely used in literature [7], [9], [11]. Namely, Gaussian and cubic *B*-spline smoothing kernel functions are considered in one and two dimensions. Validation tests are performed by considering the SPH method suitably reformulated for solving the partial differential equations (PDEs) governing electromagnetic transients [1]. The particle expressions of the Maxwell's curl equations are provided in one and two dimensions in free-space. The 2-D model is proposed for a transverse electric wave. By working with curl equations the consistency conditions must be verified by the derivatives of the unknown field functions components. Various simulations are reported with different values of the smoothing length h by considering the transient propagation of a time and space variable pulse.

The paper is organized as follows. In section 2 the background of SPH method is assumed and an analysis of the fundamental issues is reported; namely, the discrete constant and linear consistency conditions are investigated and a set of h values is determined. In section 3 the meshless formulation of the Maxwell's curl equations is provided in one and two dimensions. Simulation results referred to canonical case studies are reported.

2. Studies on the SPH method

2.1 Basic issues

In order to approximate a sufficiently regular function $f(\boldsymbol{x})$ in a domain $\Omega \subseteq \mathbb{R}^d$ by means of a convolution function $f^h \equiv f * W$ the numerical technique known as SPH adopts the so-called *kernel approximation* [6], [10], [11]:

(1)
$$f^h(\boldsymbol{x}) = \int_{\Omega} f(\boldsymbol{y}) W(\boldsymbol{x} - \boldsymbol{y}, h) d\boldsymbol{y} .$$

In (1) the function W is the *smoothing kernel function* depending on the spatial variables and on the *smoothing length* parameter h:

(2)
$$W(\boldsymbol{x} - \boldsymbol{y}, h) = \alpha_d K(\mathrm{R}),$$

where $\mathrm{R} = \|\boldsymbol{x} - \boldsymbol{y}\| / h$ and α_d is a dimension-dependent normalization constant. The smoothing kernel function is assumed to be even, normalized and with compact support [6], [10], [11]. The smoothing length h defines the size of the support.
The discrete formulation of (1) is generated by involving points, or particles, in which the function is supposed known :

(3)
$$f^h(\boldsymbol{x}) \cong \sum_{j=1}^{N} f_j W(\boldsymbol{x} - \boldsymbol{x}_j, h) V_j ,$$

where $\boldsymbol{x}_j$ are particles falling within the support of W of a fixed particle $\boldsymbol{x}$, V_j is the measure of the domain surrounding the particle $\boldsymbol{x}_j$ and $f_j \equiv f(\boldsymbol{x}_j)$. The (3) is called as *particle approximation* of f.
The spatial operator derivatives also can be approximated by means of (1). For instance, for the gradient operator on f, ∇f, under the hypotheses on f and W over reported, $(\nabla f) * W = f * (\nabla W)$. Therefore, the essential idea behind the SPH method is to approximate the spatial derivative of a function f by basing only on its knowledge on the particles, i. e. :

(4)
$$\nabla^h f(\boldsymbol{x}) \cong -\sum_{j=1}^{N} f_j \nabla W(\boldsymbol{x} - \boldsymbol{x}_j, h) V_j .$$

With some trivial manipulations, similar relations can be obtained for the divergence and the curl operators.

2.2 About the smoothing kernel function

The choice of a smoothing kernel function W must be dictated by the requirements of accuracy, smoothness, compact supportness and computational efficiency.
A normalized smoothing kernel function guarantees that the kernel approximation is at least of 1-*st* order of accuracy, $O(h)$; the requirement of evenness gives rise to the second order of accuracy. Moreover, at least the first derivative of W should be continuous so that derivatives can be computed.

In approximating a function and/or its differential operators the minimum discretization error is with evenly spaced particles. For instance, the error for the *n-th* order derivative of a function is of $O(h^{-n}(\Delta x/h)^2)$ where Δx is the interparticle spacing [2], [5], [8]. Hence, the smoothing length h must be chosen closely near to Δx to achieve the best resolution. The number $N \cong h/\Delta x$ of neighbours of a fixed particle also influences the discretization error; furthermore, the smoothing kernel function should be negligible if $R > \sigma$ where σ is a scale factor which must be suitable fixed, otherwise too many or few particles contribute to local properties.
A good choice is the Gaussian smoothing kernel function which is sufficiently smooth even for high orders of derivative but it is not really compact as it never goes to zero theoretically [6], [10], [11]:

$$K(R) = \exp(-R^2) \tag{5}$$

and α_d equals $1/\pi^{1/2}h, 1/\pi h^2, 1/\pi^{3/2}h^3$ respectively in one, two and three dimensions.
However, it is computationally very expensive since it can have a large support with an inclusion of more particles in the approximation (3), [6].
An improvement of the computational efficiency is obtained with *B*-spline compactly supported functions as smoothing kernel functions. The cubic *B*-spline function frequently used in SPH is [6]:

$$K(R) = \begin{cases} \frac{2}{3} - R^2 + \frac{1}{2}R^3 & 0 \le R < 1 \\ \frac{1}{6}(2-R)^3 & 1 \le R < 2 \\ 0 & R \ge 2 \end{cases} \tag{6}$$

and α_d equals $1/h, 15/7\pi h^2, 3/2\pi h^3$ respectively in one-, two- and three-dimensional space.
For each smoothing kernel function the smoothing length must be opportunely defined so that a good approximation could be achieved. To this aim the consistency of the computational process must be opportunely taken into account. In the following section some ideas on this topic are provided.

2.3 Consistency and reproducing conditions

The consistency conditions for SPH approximation can be expressed as its ability to exactly reproduce a polynomial up to the *k*-th order so that the approximation is said to have the *k*-th order of consistency [2], [3], [6], [7]. The polynomial reproducing conditions can be expressed by involving the particle approximation as follows:

$$\sum_{j=1}^{N} (\boldsymbol{x} - \boldsymbol{x}_j)^k W(\boldsymbol{x} - \boldsymbol{x}_j, h) V_j = \delta_{k0} \qquad k = 0,1,... \tag{7}$$

where δ is the Kronecker symbol. When the gradient operator must be approximated these conditions include the kernel derivatives. In the following the constant and linear derivative polynomial reproducing conditions are reported:

(8) $$\sum_{j=1}^{N} \nabla_i W(\boldsymbol{x}-\boldsymbol{x}_j,h)V_j = 0 \qquad i=1,\ldots,d$$

(9) $$\sum_{j=1}^{N} (\boldsymbol{x}-\boldsymbol{x}_j)_r \nabla_i W(\boldsymbol{x}-\boldsymbol{x}_j,h)V_j = \delta_{ir} \qquad i,r=1,\ldots,d$$

where $\nabla_i W$ are the smoothing kernel function derivatives with respect to the *i*-th component of the vector $(\boldsymbol{x}-\boldsymbol{x}_j)\in\mathbb{R}^d$.

The smoothing length choice is related to the reproducing conditions also: for each smoothing kernel function more than one value of *h* could satisfy the conditions (7) giving rise to a set of smoothing length *h* values.

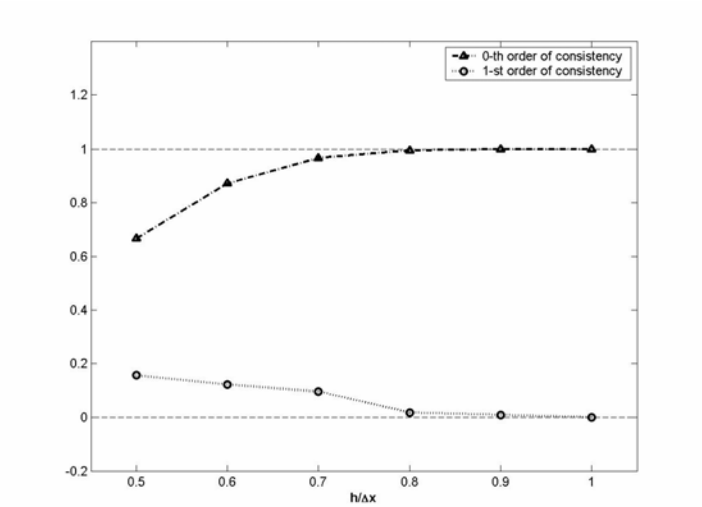

Fig. 1 Set of *h* values by using conditions (7) for the cubic *B*-spline smoothing kernel function in 1-D.

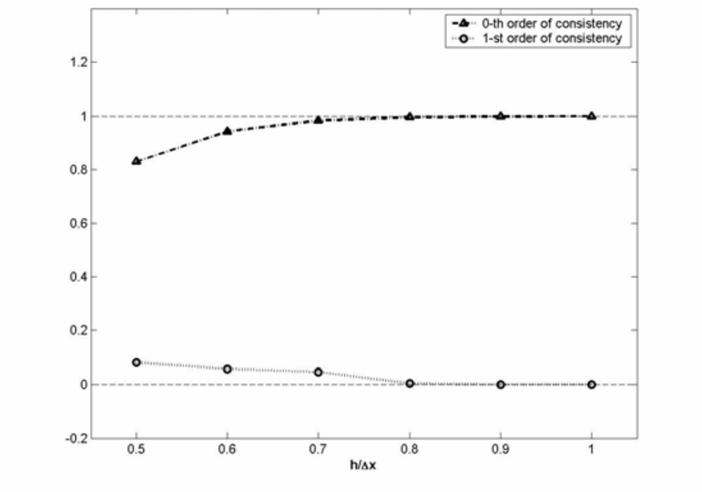

Fig. 2 Set of *h* values by using conditions (7) for the Gaussian smoothing kernel function in 1-D.

For instance, in figs. 1 and 2 the set of *h* values is depicted by using the Gaussian smoothing kernel function and the cubic *B*-spline smoothing kernel function in one

dimension and by considering an even interparticle spacing Δx. The scale factor $\sigma = 4$ is chosen for the Gaussian smoothing kernel function and it will be used from now on.
For the bell-shaped smoothing kernel functions reported the set of h values is nearly close, $h/\Delta x \in [0.8, 1.0]$, but the computational efficiency is better by using the cubic *B*-spline smoothing kernel function which involves a lesser amount of neighbours particles.

3. Numerical investigations

In this section, the SPH methodology is used to numerically achieved the time-domain electric and magnetic fields. In this context a "particle" is generalized to mean an electromagnetic field point.
In order to better clarify the main features of the method applied to electromagnetic phenomena, let us consider the time-dependent Maxwell's curl equations in free space:

$$\begin{aligned} \nabla \times \boldsymbol{H} &= \varepsilon_0 \frac{\partial \boldsymbol{E}}{\partial t} \\ \nabla \times \boldsymbol{E} &= -\mu_0 \frac{\partial \boldsymbol{H}}{\partial t}, \end{aligned} \tag{10}$$

where $\boldsymbol{E}$ and $\boldsymbol{H}$ are the electric and magnetic vector fields, ε_0 is the vacuum permittivity and μ_0 is the vacuum permeability.
The equations (10) in the 1-D formulation can be written as:

$$\begin{aligned} \frac{\partial E_x}{\partial t} &= -\frac{1}{\varepsilon_0} \frac{\partial H_y}{\partial z} \\ \frac{\partial H_y}{\partial t} &= -\frac{1}{\mu_0} \frac{\partial E_x}{\partial z}, \end{aligned} \tag{11}$$

by supposing the electric field oriented in the x direction, the magnetic field in the y direction, and the space variation accounted for the z direction.
In 2-D, a simple canonical case can be obtained by considering as case study the transverse electric field (TE). Equations (10) become:

$$\begin{aligned} \frac{\partial E_z}{\partial t} &= \frac{1}{\varepsilon_0} \left(\frac{\partial H_y}{\partial x} - \frac{\partial H_x}{\partial y} \right) \\ \frac{\partial H_y}{\partial t} &= \frac{1}{\mu_0} \frac{\partial E_z}{\partial x} \\ \frac{\partial H_x}{\partial t} &= -\frac{1}{\mu_0} \frac{\partial E_z}{\partial y}, \end{aligned} \tag{12}$$

where $E = E_z(x, y, t)$ and the same for the x and y components of the magnetic field $\boldsymbol{H}$.
The discretized expressions of (11) and (12) are obtained by employing the SPH particle approximation and the leapfrog scheme for space and time integration respectively. Namely, the equations (11) are reformulated as:

$$E_x^{n+1/2}(r_i^E) \cong E_x^{n-1/2}(r_i^E) + \frac{\Delta t}{\varepsilon_0}\sum_{j=1}^{N} H_y^n\left(r_j^H\right)\frac{\partial W\left(r_i^E - r_j^H, h\right)}{\partial r_i^E} V_j$$

(13)

$$H_y^{n+1}(r_i^H) \cong H_y^n(r_i^H) + \frac{\Delta t}{\mu_0}\sum_{j=1}^{N} E_x^{n+1/2}\left(r_j^E\right)\frac{\partial W\left(r_i^H - r_j^E, h\right)}{\partial r_i^H} V_j ,$$

where the magnetic field is computed at whole time steps n and n+1 whilst the electric field is calculated at half time steps n-1/2 and n+1/2, [12], [13]. Moreover, the particles r_k^E and r_k^H involved in the formulas are particles fixed for the $\boldsymbol{E}$ and $\boldsymbol{H}$ fields respectively.
In the same manner, the discretization in space and time of equations (12) is expressed by means of the following formulas:

$$E_z^{n+1/2}(\boldsymbol{r}_i^E) \cong E_z^{n-1/2}(\boldsymbol{r}_i^E) +$$
$$+ \frac{\Delta t}{\varepsilon_0}\sum_{j=1}^{N}\left[H_y^n\left(\boldsymbol{r}_j^H\right)\nabla_x W\left(\boldsymbol{r}_i^E - \boldsymbol{r}_j^H, h\right) - H_x^n\left(\boldsymbol{r}_j^H\right)\nabla_y W\left(\boldsymbol{r}_i^E - \boldsymbol{r}_j^H, h\right)\right] V_j$$

(14)

$$H_y^{n+1}(\boldsymbol{r}_i^H) \cong H_y^n(\boldsymbol{r}_i^H) + \frac{\Delta t}{\mu_0}\sum_{j=1}^{N} E_z^{n+1/2}\left(\boldsymbol{r}_j^E\right)\nabla_x W\left(\boldsymbol{r}_i^H - \boldsymbol{r}_j^E, h\right) V_j$$

$$H_x^{n+1}(\boldsymbol{r}_i^H) \cong H_x^n(\boldsymbol{r}_i^H) - \frac{\Delta t}{\mu_0}\sum_{j=1}^{N} E_z^{n+1/2}\left(\boldsymbol{r}_j^E\right)\nabla_y W\left(\boldsymbol{r}_i^H - \boldsymbol{r}_j^E, h\right) V_j .$$

The time integration is subjected to the Courant-Friedrichs-Levy (CFL) stability condition [12], [13] requiring the time step to be proportional to the spatial resolution and, consequently, to the smoothing length h.

3.1 One-dimensional case study

By working with the Maxwell's curl equations the polynomial reproducing conditions must be imposed on the derivatives of the field functions components in order to recognize the set of smoothing length h values.
In fig. 3 the set of h values carried out by the condition (9) is provided for the derivatives of the cubic B-spline and the Gaussian smoothing kernel functions. The 0-*th* order of consistency is always satisfied.

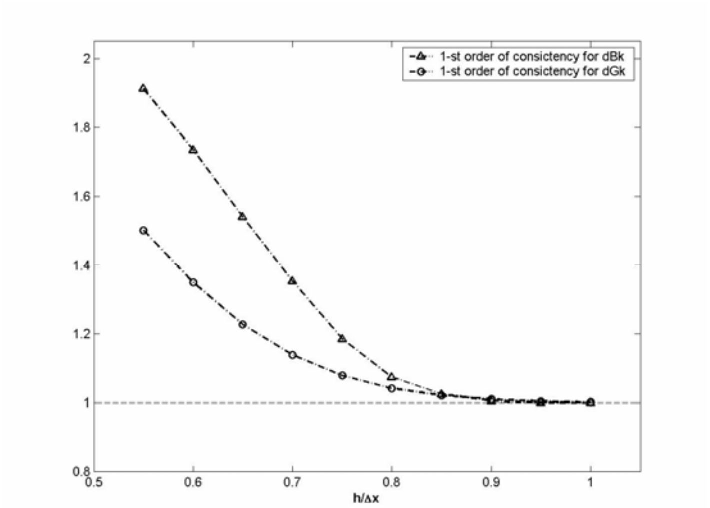

Fig. 3 Set of *h* values for derivatives of the cubic *B*-spline (dBk) and the Gaussian (dGk) smoothing kernel functions in one-dimension.

The equations (13) are used in simulating the transient propagation of the following time variable pulse centered in the spatial domain that is of 3.83 m:

(15) $$E_{x0}(t) = \sin(\pi f_0 t)$$

where the excitation frequency is $f_0 = 7$ MHz. The particles are evenly spaced with the interparticle spacing equal to $\lambda / 20$, where λ is the wave length. The electric field is normalized both in 1-D and 2-D simulations in order to be comparable in value with the magnetic field. In fig. 4 the evolution of the space profile of the propagating pulse of the electric field is depicted by choosing $h = 0.92 \cdot \Delta x$ as smoothing length for the cubic *B*-spline smoothing kernel function and the Gaussian smoothing kernel function.

In figs. 5 and 6 the behaviour of the electric field is shown by fixing $h = 0.6 \cdot \Delta x$ and $h = 1.2 \cdot \Delta x$, respectively. In fig. 5 the strongly smoothed behaviour of the space profile is due to the insufficient number of neighbours particles arising from *h* lower than Δx; on the contrary, the noise in fig. 6 is generated by the high number of neighbours particles arising from Δx far from *h*.

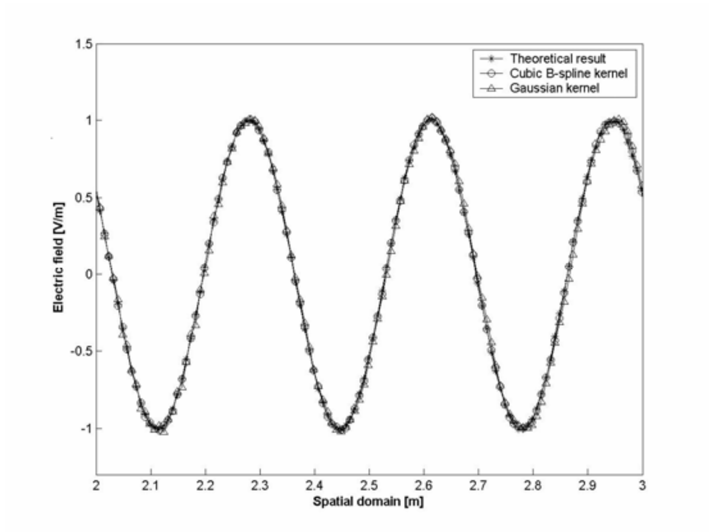

Fig. 4 Comparison among the space profiles of theoretical propagating pulse and SPH simulations using the cubic *B*-spline and the Gaussian smoothing kernel functions with h=0.92·Δx.

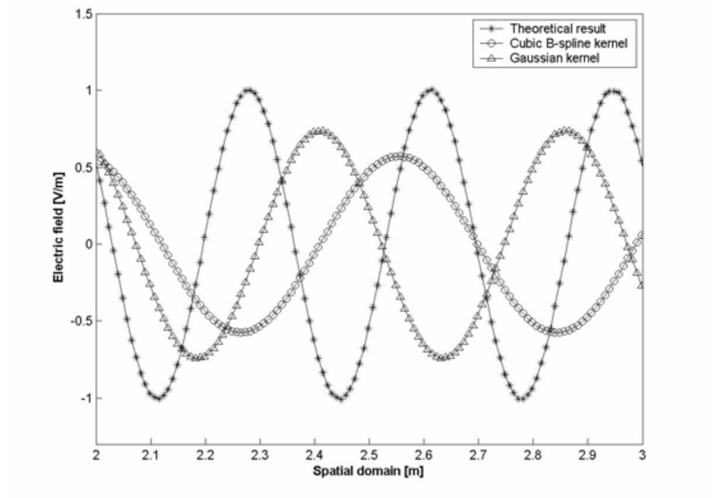

Fig. 5 Comparison among the space profiles of theoretical propagating pulse and SPH simulations using the cubic *B*-spline and the Gaussian smoothing kernel functions with h=0.6·Δx.

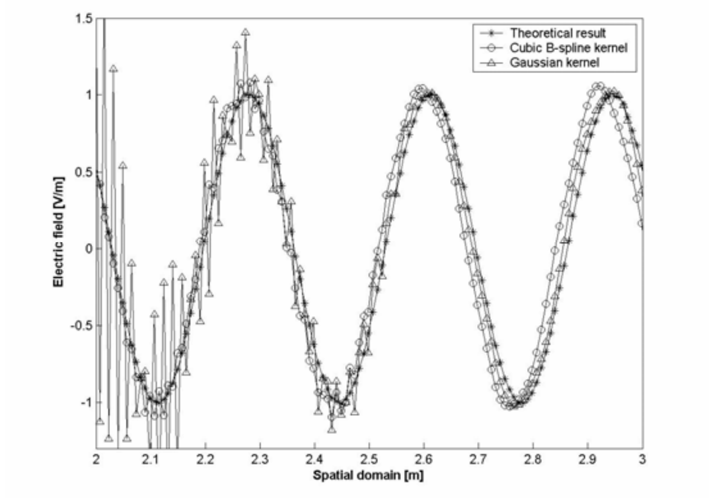

Fig. 6 Comparison among the space profiles of theoretical propagating pulse and SPH simulations using the cubic *B*-spline and the Gaussian smoothing kernel functions with h=1.2·Δx.

3.2 Two-dimensional TE wave simulations

In $\mathbb{R}^2$ the constant and linear derivative polynomial reproducing conditions (8) and (9) are:

$$\sum_{j=1}^{N} \nabla_1 W(\boldsymbol{x}-\boldsymbol{x}_j,h)V_j = \sum_{j=1}^{N} \nabla_2 W(\boldsymbol{x}-\boldsymbol{x}_j,h)V_j = 0 \tag{16}$$

$$\sum_{j=1}^{N} (\boldsymbol{x}-\boldsymbol{x}_j)_1 \nabla_1 W(\boldsymbol{x}-\boldsymbol{x}_j,h)V_j = \sum_{j=1}^{N} (\boldsymbol{x}-\boldsymbol{x}_j)_2 \nabla_2 W(\boldsymbol{x}-\boldsymbol{x}_j,h)V_j = 1 \tag{17}$$

$$\sum_{j=1}^{N} (\boldsymbol{x}-\boldsymbol{x}_j)_1 \nabla_2 W(\boldsymbol{x}-\boldsymbol{x}_j,h)V_j = \sum_{j=1}^{N} (\boldsymbol{x}-\boldsymbol{x}_j)_2 \nabla_1 W(\boldsymbol{x}-\boldsymbol{x}_j,h)V_j = 0 \tag{18}$$

and they provide the set of h values.
By working with the cubic *B*-spline smoothing kernel function, the 0-*th* order of consistency is verified when $0 < h/\Delta x \le 0.8$; the 1-*st* order is verified for $0.53 < h/\Delta x \le 0.55$ as shown in fig. 7 depicting the $h/\Delta x$ values for the (17) and (18) conditions. In the same manner, the values of h fall in $(0, 0.68]$ for 0-*th* order, and in $[0.382, 0.386]$ for 1-*st* order of consistency by using the Gaussian smoothing kernel function (fig. 8).

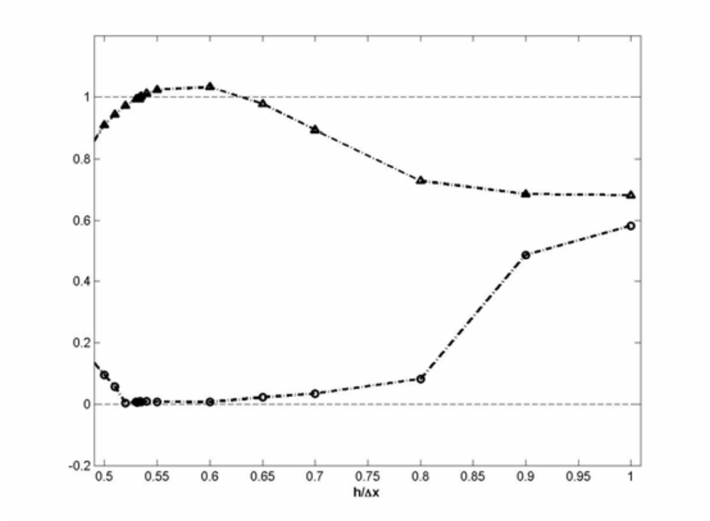

Fig 7 Set of *h* values for the cubic *B*-spline smoothing kernel function in two-dimension.

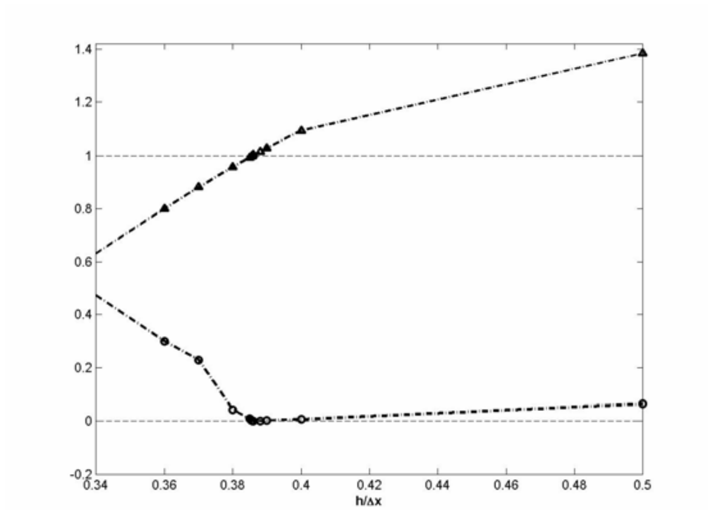

Fig. 8 Set of *h* values for the Gaussian smoothing kernel function in two-dimension.

The transient evolution of a time variable E_z field turned-off after the second time step is simulated:

(15) $$E_{x0}(t) = \frac{10}{\|\boldsymbol{x}\|_2} \sin\left(2\pi f_0 t + \frac{2\pi f_0 t}{c_0}\|\boldsymbol{x}\|_2\right)$$

where $f_0 = 20$ MHz and c_0 is the speed of light in free space. The square domain $\Omega = [0, 40] \times [0, 40]$ is arranged by evenly spaced particles with $\Delta x = \Delta y = 0.1$.

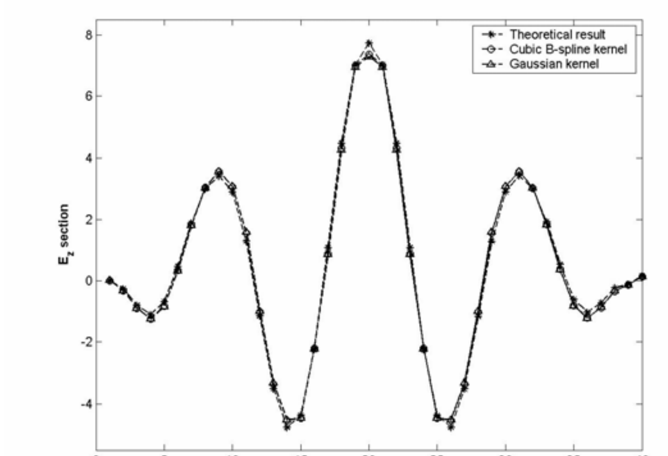

Fig. 9 Section of space profiles of the electric field E_Z at time step *t*=20.

In fig. 9 the computed space profile of the electric field E_Z on a plane $y = const$ is shown in comparison with the theoretical result at a fixed time step. The SPH simulations are with the cubic *B*-spline smoothing kernel function and the Gaussian smoothing kernel function, respectively. The experiments are performed by fixing the smoothing length $h = 0.534 \cdot \Delta x$ and $h = 0.385 \cdot \Delta x$, for the two smoothing kernel functions respectively. In figs. 10, 11, 12 the space profiles of the electric field is reported too. A good agreement has been reached.

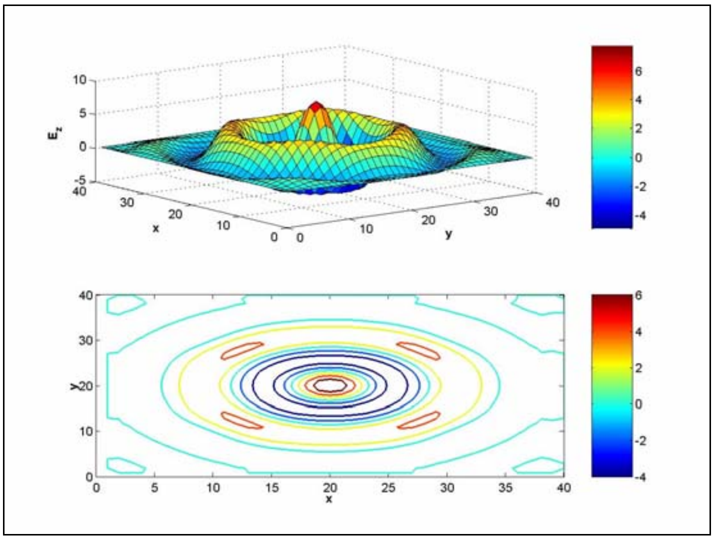

Fig. 10 Theoretical expected result for the electric field E_Z.

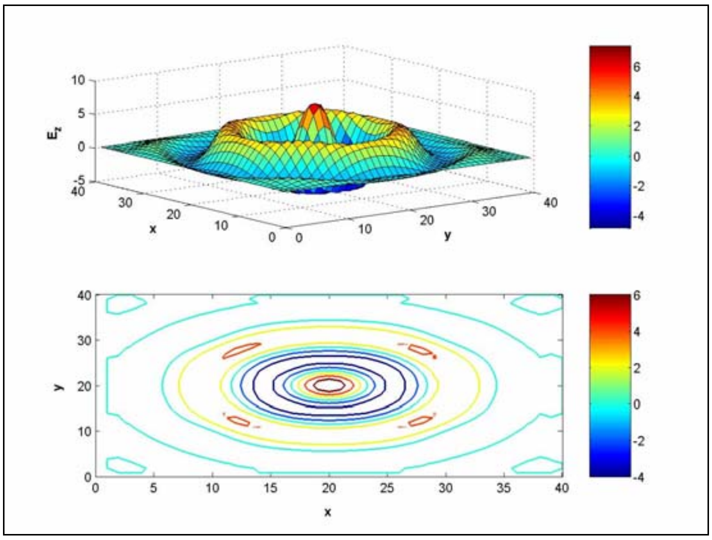

Fig. 11 Computed result with the cubic *B*-spline smoothing kernel function for the electric field E_Z.

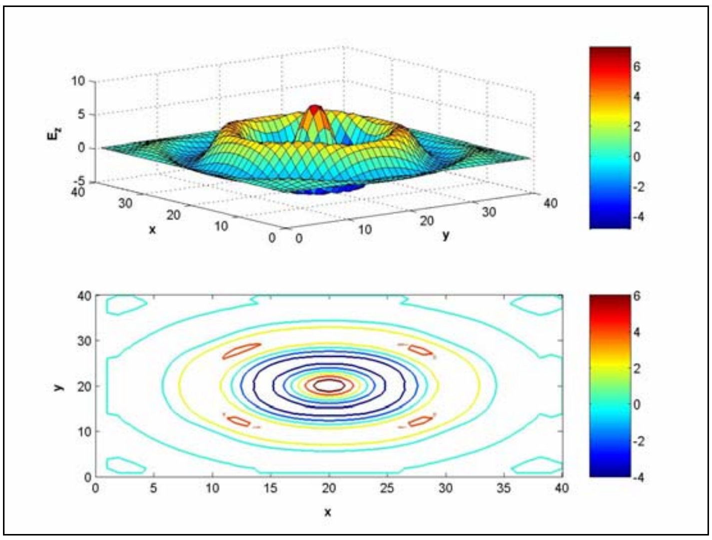

Fig. 12 Computed result with the Gaussian smoothing kernel function for the electric field E_Z.

4. Conclusions

This paper provides an objective method, based on the polynomial reproducing conditions, to determine a set of values of the smoothing length *h* to achieve a good SPH approximation of the unknown field functions. Two bell-shaped smoothing kernel functions, i.e. the cubic *B*-spline and the Gaussian smoothing kernel functions, have been taken into account. At first, the criterion has been adopted to recognize proper *h* values verifying the constant and linear consistency conditions. Moreover, the consistency has been analyzed for the curl differential operator. Numerical investigations have been performed on Maxwell's curl equations in free space for 1-D and 2-D formulations. By considering the *h* values recognized by means of the described criterion, a good agreement has been obtained in comparison with the theoretical expected results.

REFERENCES

[1] Ala G., Francomano E., Tortorici A., Toscano E. and Viola F., A smoothed particle interpolation scheme for transient electromagnetic simulation, *IEEE Transaction on Magnetics*, (2005), to appear.

[2] Belytschko T., Krongauz Y., Dolbow J. and Gerlach C., On the completeness of meshfree methods, *International Journal for Numerical Methods in Engineering*, **43**, pp. 785-819 (1998).

[3] Bonet J. and Lok T.-S. L., Variational and momentum preservation aspects of Smooth Particle Hydrodynamics formulations, *Computer methods in applied mechanics and engineering*, **180**, pp. 97-115, (1999).

[4] Gingold R. A. and Monaghan J. J., Smoothed particle hydrodynamics: theory and application to nonspherical stars, *Monthly Notices of the Royal Astronomical Society*, **181**, pp. 375-389 (1985).

[5] Laguna P., Smoothed particle interpolation, *The Astrophysical Journal*, **439**, pp. 814-821 (1994).

[6] Liu G. R. and Liu M. B., Smoothed particle hydrodynamics - a mesh-free particle method, *World Scientific Publishing,* (2003).

[7] Liu M. B., Liu G. R. and Lam K. Y., Constructing smoothing functions in smoothed particle hydrodynamics with applications, *Journal of Computational and Applied Mathematics,* **155**, issue 2, pp. 263-284 (2003).

[8] Mas-Gallic S. and Raviart P. A., A Particle Method for First-order Symmetric Systems, *Numerische Mathematik*, **51**, pp. 323-352 (1987).

[9] Monaghan J. J. and Lattanzio J. C., A refined particle method for astrophysical problems, *Astronomy and Astrophysics*, **149**, pp. 135-143 (1985).

[10] Monaghan J. J., An introduction to SPH, *Computer Physics Communicatios,* **48**, pp. 89-96 (1988).

[11] Monaghan J. J., Smoothed particle hydrodynamics, *Annual Review of Astronomical and Astrophysics,* **30**, pp. 543-574 (1992).

[12] Sullivan D. M., Electromagnetic simulation using the FDTD method, *IEEE press*, (2000).

[13] Taflove A. and Hagness S., Computational Electrodynamics: The Finite-Difference Time-Domain Method, *Artech House,* Boston, (2000).